JOURNAL OF Materials CHEMISTRY

Sorption behaviour of uranium on birnessite, a layered manganese oxide

Lina Al-Attar and Alan Dyer*

Cockcroft Building, School of Science, University of Salford, Salford, UK M5 4WT

Received 21st September 2001, Accepted 28th January 2002
First published as an Advance Article on the web 2nd April 2002

Birnessite, a layered manganese oxide material, its corresponding cation-exchanged forms and their autoclaved samples were investigated for their ability to take up uranium using the batch method. Uranium sorption was also studied on these materials as a function of uranium solution pH. Batch distribution factor (K_d) and percentage sorption were used as selectivity factors to assess uranium sorption.

Introduction

Uranium is one of the most toxic heavy metals. Its contamination results from the nuclear industry and poses a threat in surface and ground waters.[1] The investigation of the interaction of uranium and other actinides with inorganic microporous ion-exchange materials is an important target for the nuclear industry because of the suitability of these materials for the treatment of liquid effluents and final storage of radioactive wastes. Inorganic ion exchangers have a number of advantages making them preferable to the organic ones; they have been found to be highly resistant towards radiation damage, and to have high thermal and chemical stability. They also often show very high cation-exchange selectivities.

Manganese octahedral molecular sieves (OMS) with layered and tunnel structures have attracted considerable interest due to their potential application in separation. This new class of materials has shown unique ion-sieve properties for the adsorption of metal ions.[2]

Among these materials are todorokite and birnessite, its precursor. Birnessite is the most common stable layered manganese oxide mineral. Jones and Milne[3] were the first to report its occurrence in the Birness Region (Scotland). It is the main Mn-bearing phase in soil, marine manganese nodules and micro-nodules and has a unique surface charge,[4] cation-exchange[5] and redox[6] properties. It can behave as an ion-sieve material with an effective pore diameter of 3 Å,[7] and a preference towards heavy metals that plays a significant role in their distribution, particularly cobalt, in soil and marine environments.

Natural birnessites often contain Co^{2+}, Ni^{2+} and Ba^{2+} in appreciable quantities.[8] They exhibit no ion exchange due either to their preference for these cations or to chemical changes undergone during dehydration.[9]

The structure of Na-birnessite consists of two-dimensional sheets of edge-shared MnO_6 octahedra separated by exchangeable Na ions in a single water molecule sheet.[10] The basal spacing of this mineral is 7 Å in the dry state. Na-birnessite results from the dehydration of buserite. Buserite has basal spacing of about 10 Å, and contains two-dimensional sheets of edge-shared MnO_6 octahedra with double-water molecule sheets between the sheets of the shared MnO_6 octahedra and Na^+ sheets between the water sheets.[11] Since Na^+ hydration is weak, the waters in Na-buserite (basal spacing *ca.* 10 Å) are easily lost, transforming the buserite structure to birnessite (basal spacing *ca.* 7.1 Å) after drying. A synthetic analogue of the natural occurring birnessite manganese oxide mineral, can be prepared under controlled laboratory conditions, the formula of the Na-form being $Na_4Mn_{14}O_{26}{\cdot}9H_2O$, which is non-stoichiometric.

Todorokite-type manganese oxide material has a one-dimensional (3 × 3) tunnel structure and acts as a molecular sieve with a pore size of 6.9 Å.[12] Monovalent, divalent metal ions and water molecules were found to occupy the (3 × 3) tunnel sites[13] in a natural todorokite that originated from manganese nodules found in different localities. Mg^{2+}, Co^{2+}, Ni^{2+}, Cu^{2+} and Zn^{2+} cations coordinated with six water molecules have a size similar to the tunnel size of todorokite (*ca.* 6.9 Å),[11] and they often form isostructural materials with spinel, CdI_2 and $Mn(OH)_2$ structures. Because of this, Mg^{2+}, Co^{2+}, Ni^{2+}, Cu^{2+}, and Zn^{2+} cations have been suggested as good templates for the transformation of buserite into todorokite-like materials.[11] Natural todorokite of high purity is rare, poorly crystalline, and coexists with other manganese oxide minerals. Applications of natural todorokite have, therefore, been limited.

Mg-exchanged buserite keeps the double-water structure after drying, due to the strong affinity of Mg^{2+} for water.[2] The size of the hydrated Mg^{2+} just fits the (3 × 3) tunnel of the todorokite structure so Mg-buserite can be transformed to todorokite by hydrothermal treatment.[14] This synthetic todorokite manganese oxide material has a much higher Mg^{2+} content than the natural form.

Golden *et al.*[10] have reported a synthetic todorokite prepared by hydrothermal treatment of Mg-exchanged birnessite. Shen *et al.*[12] have developed a thermally stable todorokite and found that the exchange capacity of this material depended on the nature of the cations, the ageing temperature and drying treatment. Consequently, the nature of the metal ions present in the tunnels is important to the application of todorokites.

In this work the potential application of birnessite, its cation-exchanged forms and their autoclaved forms was investigated for the uptake of uranium. The influence of uranium solution pH was also considered in order to explain the nature of the sorption mechanism of uranium onto these materials. It is known that the sorption of actinides on microporous materials is influenced by the solution pH, and that hydrolysis products of the actinides are important solution species.[15,16]

Experimental

Chemicals

All chemical reagents used in this work were of analytical reagent grade and obtained from chemical commercial suppliers.

Natural uranyl nitrate $UO_2(NO_3)_2 \cdot 6H_2O$, supplied by B.D.H. Ltd, was the uranium source used.

Preparation of Na-birnessite sample

Birnessite was synthesised by adding 250 mL of 5.5 M NaOH to 200 mL of 0.5 M $MnCl_2$, at room temperature, in a plastic beaker. Oxygen was then bubbled at a rate of $\geqslant 1.5$ L min^{-1} through a glass frit into the $Mn(OH)_2$ suspension with vigorous stirring. It was important to maintain this rate of oxygen flow to prevent the formation of hausmannite, Mn_3O_4. The oxygenation was stopped after 5 hours and the black precipitate of birnessite was collected and washed several times with deionised water until it was salt free. The final product was air-dried.

Preparation of cation-exchanged birnessite samples and their autoclaved forms

Na-birnessite was converted to other metal-ion forms by ion-exchanging 2 g several times with 200 mL (1 M) of the inorganic salt of the appropriate cation, *i.e.* $MgCl_2$, $Ni(NO_3)_2$, $CoCl_2$, $CsNO_3$, $Ca(NO_3)_2$, $BaCl_2$, KNO_3, $LiNO_3$, $CuCl_2$ and $ZnCl_2$[1] in 250 mL polycarbonate bottles, with stirring, for 6 hours at ambient temperature .One gram of each ion-exchange suspension was then washed several times with deionised water and air-dried. The remainder was suspended in deionised water, placed into Teflon-lined, sealed, stainless steel vessels and autoclaved under autogenous pressure at 155 °C for 8 hours. The vessels were cooled to room temperature and the suspensions were filtered, washed several times with deionised water, and air-dried.

Autoclaving time was limited to 8 hours since it had previously been noted[10] that prolonged autoclaving caused the gradual appearance of manganite (γ-MnOOH). This indicated that some Mn^{2+} ions had been expelled from birnessite, or todorokite, into the solution and had precipitated as manganite.

Physical analysis

Powder X-ray diffraction (XRD) patterns of the synthetic birnessite, cation-exchanged birnessites and their autoclaved forms were collected on a Siemens D5000 diffractometer with Cu-Kα radiation. Operation conditions were $\lambda = 1.54179$ Å, 2θ range 6–50, step size 0.02°, time 10 s $step^{-1}$, $T = 293$ K). The X-ray diffractometer was always operated under the same conditions (incident slits 0.6 and 2 mm, 40 V and a current of 40 mA). All samples were analysed within a two week period. The water contents in samples pre-equilibrated over saturated NaCl for a week were determined by thermogravimetry (TGA) using a Mettler TA3000 system at a heating rate of 5 K min^{-1} in the range 298–973 K under a nitrogen atmosphere.

Chemical analysis

Elemental chemical analyses of cation-exchanged forms of birnessite were performed using an S11 AA/AE Spectrophotometer. About 15–40 mg of the sample were dissolved in a mixture of 0.5 mL concentrated HCl (37%, Fisher) and 1 drop of 30% W/V (Fisher) hydrogen peroxide solution. The colourless solutions were analysed after dilution. Table 1 summarises the extent of exchange in their dehydrated forms.

Sorption experiments

The sorption of uranium was performed using a batch method. 30 mg of the M-birnessite (where M is the exchanged cation) were stirred at ambient temperature with 6 mL (*i.e.*, $V/M = 200$ mL g^{-1}) of a uranium solution (250 mg L^{-1}) in 15 mL polyethylene centrifuge tubes (Elkay) using a mineralogical roller. Contact time was varied between 0.5 to 8 hours. All the sorption experiments, except when the pH was varied, were at pH = 3–3.5, which was that obtained at $V/M = 200$ mL g^{-1}. The solutions were separated from the solids using a Centaur MSE-2 (Orme) centrifuge (5–15 min at 4000 *g*), followed by filtration through a 0.2 μm PVDF membrane (Whatman). The pH of the filtrates was recorded using an Orion model 720A pH meter fitted with an Accumant semi micro-calomel electrode.

Table 1 The percentage of cation exchange (M) in birnessite

M-birnessite	% Exchange
Li	27
K	100
Cs	86
Ba	67
Co	85
Cu	97
Zn	58
Ca	82
Mg	121
Ni	133

Alpha activity of uranium solutions was determined in a liquid scintillation counter provided with pulse shape analysis (PSA) to eliminate the interference of beta radiation from its daughter ^{234}Th. Efficiency for alpha counting was assumed to be 100%.[17] Two major uranium peaks were observed, at 4.268 MeV (^{238}U) and 4.793 MeV (^{234}U).[18] They were equal in the area as the two isotopes were in secular equilibrium. A minor peak at 4.681 MeV, not fully resolved, was attributed to ^{235}U. The energy range used for uranium determinations was 150–400 keV. Counting was carried out for a sufficient period of time to attain 1–2% statistical accuracy. Blank experiments showed negligible uranium sorption on the walls of vials and centrifuge tubes. Reference experiments were also run to represent the initial uranium activity.

The amount of uranium sorbed on the manganese oxide materials was expressed in terms of a batch distribution coefficient (K_d), defined as:

$$K_d = \left(\frac{A_i - A_t}{A_t}\right) \times \frac{V}{M} = \frac{Concentration\ of\ ion\ in\ exchanger}{Concentration\ of\ ion\ in\ solution} \quad (1)$$

A_i and A_t are the initial and final uranium activity respectively, and V/M is the ratio of solution volume to exchanger mass (*i.e.* batch factor/mL g^{-1}). K_d values were based on the hydrated mass of the exchanger. Percentage sorptions were also calculated.

The influence of uranium solution pH on uranium uptake

The effect of uranium solution pH was examined within the range pH 1–12. Uranium solutions of constant concentration (250 mg L^{-1}) at a batch factor of 200 mL g^{-1} were used throughout. Solution–solid contact time was 4 hours, less than that at which equilibrium had been achieved.

Results and discussion

Synthesis

Powder XRD patterns of Ca, Ni and Mg cation-exchanged samples (Table 2) had their strongest peaks at *d* spacings of 9.98, 9.81, and 9.82 Å respectively, and were assigned to buserite (indicating the hydration of birnessite to buserite). The slight variation in *d* corresponded to in-going cation size. When other cations were exchanged into Na-birnessite no reflections in the range 9.9–9.6 Å were found (Table 3). The peak at ~7.1 Å due to Na-birnessite was retained which was in agreement with earlier observations.[9,12]

Peak intensity and sharpness varied from sample to sample. For some samples the peak at ~7.1 Å was strong and sharp.

Table 2 *d* Spacings from XRD powder patterns of un-autoclaved cation-exchanged buserites (Å)

Cation		
Ca	Mg	Ni
9.98	9.82	9.81
7.29		7.77
5.02	4.84	4.86
3.47	3.22	3.23
2.58	2.55	2.58
2.47	2.49	2.50
2.42	2.43	2.42
	2.36	2.30
2.12	2.10	2.22

Table 3 *d* Spacings from powder XRD patterns of un-autoclaved cation-exchanged birnessites (Å)

Cation							
Na	Li	K	Cs	Ba	Cu	Co	Zn
7.13	7.13	7.10	7.38	7.12	7.34	7.33	7.25
					5.51		
3.56	3.56	3.53	3.68	3.54	3.64	3.60	3.61
2.52	2.52	2.75	2.54	2.52	2.77		
		2.48	2.48	2.48	2.46	2.47	2.46
2.43	2.43	2.42	2.42	2.42	2.33	2.34	2.33
2.22	2.22	2.26	2.25	2.27	2.28		
2.16	2.15	2.12	2.15	2.14			2.04

For others it was weak and broad indicating that, after ion exchange, the crystallinity of the layered materials, or the ordering of the cations into the interlayer, was poor. A previous study[11] on birnessites, prepared using $Mg(MnO_4)_2$ as an oxidizing reagent, and then aged for 4 days at room temperature, showed that Mg-, Ni-, Co- and Cu-exchanged materials had 9.6 Å basal spacings. Our results for Co- and Cu-birnessites were 7.33 and 7.34 Å respectively reflecting the difference in the preparation and drying methods.

Autoclaved cation-exchanged samples gave XRD patterns with the same basal spacings as those prior to autoclaving, but with broader and less intense peaks. This may be related either to a smaller particle size, a high degree of disorder in the crystallites or both.[10,11]

Upon autoclaving, the cation-exchanged birnessites with $\sim$10 Å spacings favoured the formation of (3 × 3) tunnel todorokite-like structures whereas the corresponding autoclaved birnessites having $\sim$7 Å spacings indicated changes to tunnel structures that were two octahedra wide, more typical of the (2 × 2) tunnel structure of hollandite or cryptomelane.[10] This was because, when birnessite transforms to a tunnel structure, the initial distance between the birnessite layers seems to have some control on the dimensions of the tunnels.

The powder pattern of the autoclaved Mg-exchanged sample obtained in this work was very similar to that reported by Feng *et al.*[2] in which the most intense peak was at about 10 Å. This result supported the expectation that todorokite tunnel-type materials were indeed formed by hydrothermal treatment. This differed from observations by Shen *et al.*[11] in which the second order peak at 4.8 Å was much more intense than that at 9.6 Å. In both cases, the XRD patterns were related to the tunnel todorokite-type mineral since the 9.6 and 4.9 Å *d* spacing lines in the diffraction patterns served as diagnostic peaks for todorokite.[19] Peaks at 3.19 and 2.40 Å were also recorded in natural todorokite.[12] The variation of the basal spacing of todorokite depended on the synthesis procedure and resulted in different ion exchange properties. The difference in synthesis procedure leads to variations in the Mg/Mn ratio and the mean oxidation number of Mn in Mg-todorokite.[2,14] In addition, pH, temperature, autoclaving procedure, and the nature of the cations all influence the crystallinity and consequently the cation-exchange capacity of the resultant todorokite-type material.

The autoclaved Ca-exchanged sample had an XRD pattern with broad, low intensity peaks at 9.98, 7.29 and 2.47 Å. According to HRTEM images,[10] this suggested the presence of tunnels of variable dimension in the *a* direction, which explained the disorder indicated by broad, weak XRD reflections. The XRD pattern of the autoclaved Ca-birnessite sample may indicate the existence of alternate one- and double-water sheets between the sheets of MnO_6 octahedra.

The product obtained by autoclaving Mg-birnessite had sharp, intense XRD peaks indicating a better crystalline order than in those obtained by autoclaving Ni- or Ca-birnessites.

Elemental analysis of cation-exchanged birnessite forms (Table 1)

The equilibrium pH of all the cation-exchanged experiments was in the range pH 5.1–7.7 with the exception of that for Ca-exchange which was between pH 2.8 and 5.2. This indicated that the formation of hydroxides was unlikely. An apparent excess exchange was observed in the Ni^{2+} and Mg^{2+} samples (133 and 121% respectively) which was an artefact arising from the fact that these exchanged forms had the buserite structure, *i.e.* the hydrated form of birnessite, as indicated by their powder patterns (Table 2). This meant that cation access into additional interlayer sites was possible in the buserite structures. According to literature,[20,21] the alkali and alkaline earth metal ions with large ionic radii (unhydrated) were usually located on the water sheet in the interlayer. Transition metals ions with small ionic radii (*e.g.* Zn^{2+}, Cu^{2+}, and Co^{2+}) were more likely to be located above and below the vacancies on the MnO_6 sheets.

The behaviour observed with Li^+ exchange was not unusual and arose from the high hydration of the cation. The low exchange of Zn^{2+} might be related to the fact that it behaves more like the alkali and alkaline earth metal ions. The exchange maxima of Cs^+ and Ba^{2+} reflected their large ionic size.

TGA analysis

The percentage mass loss of cation-exchanged birnessites and their autoclaved forms are summarised in Table 4.

Thermogravimetric analysis results (Fig. 1) showed that the percentage mass losses of autoclaved exchanged samples were less than those prior to autoclaving in the temperature range 298–973 K used.

The mass losses up to 600 K could be ascribed to water loss for all the cation-exchanged birnessite materials (Fig. 2). It can be seen that, as the size of the exchanging cation increased, the temperature at which the water loss occurred also increased. Two peaks appeared on the differential thermograms (DTG) for Mg-, Ni- and Ca-birnessites indicating the presence of two

Table 4 The percentage mass losses (to 973 K) of cation-exchanged birnessites (B) and their autoclaved forms (AB)

	A	AB
Li	18	14
Na	17	16
K	10	9
Cs	12	9
Mg	32	22
Ca	19	17
Ba	13	10
Co	22	20
Ni	27	22
Cu	24	21
Zn	22	20

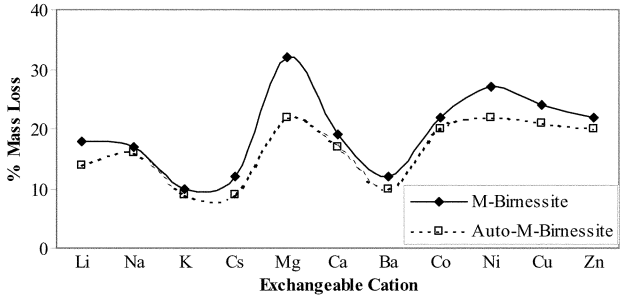

Fig. 1 Percentage mass loss of cation-exchanged birnessite sample materials and their autoclaved forms *vs.* the cation exchanged.

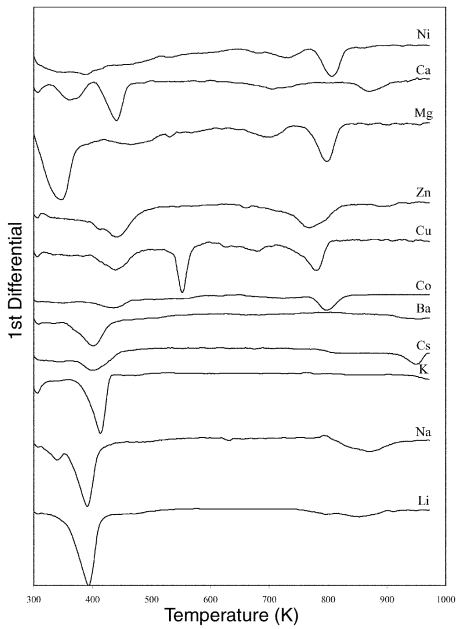

Fig. 2 DTG curves of Na-birnessite and its corresponding cation-exchanged forms, prior to autoclaving, in the temperature range 298–973 K under a nitrogen atmosphere.

water layers. Since Mg^{2+} is a strongly hydrated cation, the Mg-birnessite sample was associated with mass losses of 13.35% in the first peak and 6.40% in the second one. Similar events were 6.37 and 5.58% for Ni-birnessite, and 4.41 and 4.62% for Ca-birnessite. Mass loss peaks appeared on most of the DTG traces at temperatures above 723 K and could be ascribed to hydroxy loss.

Results of batch experiments

Un-autoclaved samples. Figs. 3a and 3b illustrate the performance of cation-exchanged birnessite samples in the sorption of uranium from aqueous solutions as solid–solution contact time increased. The performances of the corresponding autoclaved samples are in Figs. 3c and 3d.

The highest uptake of uranium was that of the Cs-exchanged birnessite with $K_d = 1.67 \times 10^6$ mL g^{-1} (100% sorption). This was higher than those obtained for the uptake of uranium on titanosilicate materials[22,23] and much higher than those obtained by Misaelides *et al.*[15] who studied the sorption of uranium onto untreated and NaCl-pretreated zeolite-bearing volcanoclastic rock samples from Metaxades (Thrace, Greece).

Li-birnessite attained a K_d value of 18.2×10^4 mL g^{-1} (99.9% sorption) after 4 hours. Na- and K-birnessites attained equilibrium more quickly and K_d values of 4.9×10^4 (99.6% sorption) and 8.8×10^4 mL g^{-1} (99.8%sorption) respectively

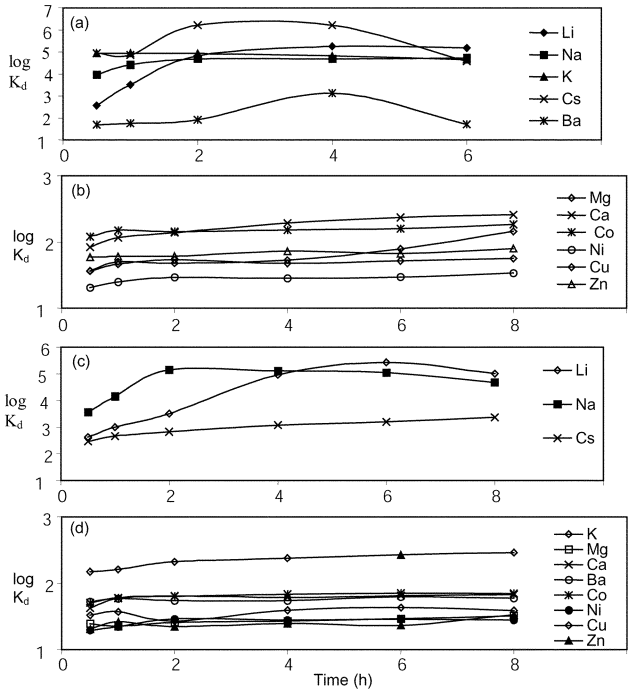

Fig. 3 Variation of K_d for uranium sorption on the non-autoclaved Na-birnessite manganese oxide materials, its cation-exchanged forms (a and b) and their autoclaved samples (c and d) as a function of equilibrium time at ambient temperature ($V/M = 200$ mL g^{-1}, [U] = 250 mg L^{-1}).

were recorded. Uranium uptakes onto alkaline earth birnessites increased solution–solid contact time but were much lower.

Golden *et al.*[9] found that the *b*-dimension in birnessite [calculated from *d*(060)] increased with cation size from the alkali and alkaline earth cations. The reason for this increase in the *b*-dimension was not clear; however, the smaller cations have relatively large charge/size ratios and are more effective in layer-charge neutralisation. Thus, an expansion in the *b*-dimension may be expected as the cation size increases. This may explain why the K_d values for uranium sorption were relatively high on Cs- and Ba-birnessites. Uranium uptakes on birnessites containing transition element cations were all low (34–184 mL g^{-1}).

Autoclaved samples. The uptake of uranium onto the autoclaved birnessites was less than that prior to autoclaving (Figs. 3c and 3d) with the exception of the Li sample which gave the maximum uranium uptake observed, reaching a K_d of 2.71×10^5 mL g^{-1} (99.9% sorption) after 6 hours' equilibrium time. Other autoclaved birnessites (K^+, Ba^{2+}, Co^{2+}, Cu^{2+}, and Zn^{2+}) had low K_d values (Fig. 3d).

Dry heating of K- and Ba-saturated birnessites has been shown to give rise to cryptomelane (tunnel size 7 Å, K^+ in the tunnels) and hollandite (tunnel size 4.6 Å, Ba^{2+} in the tunnels).[24,25] Cryptomelane or hollandite-type manganese oxide show cation-exchange properties in the aqueous phase after extraction of the metal cations in the tunnel sites.[26,27] Tsuji *et al.*[28,29] studied the ion-exchange mechanism of a hollandite-type manganese oxide with K^+ in the (2 × 2) tunnel sites in the aqueous phase. The K^+ can be topotactically extracted by 13 M HNO_3, and acid-treated cryptomelane showed high selectivities for the adsorption of K^+, Rb^+, Ba^+ and Pb^{2+}. This was interpreted as an ion-sieve effect in the (2 × 2) tunnel, which has a suitable size for fixing ions having an effective ionic radius of about 1.4 Å. This was in agreement with the study of Dyer *et al.*[30] who found cryptomelane to be very effective for the adsorption of ^{89}Sr from distilled water at

pH 4, also for ^{110}Ag (ionic radius = 1.29 Å) at a lower pH (3.4) when 99.97% sorption was noted.

The autoclaved todorokite-type samples (Ca, Ni and Mg forms) showed a low affinity for the uranyl ion, K_d = 25–60 mL g^{-1}, with low percentage sorption. This could be related to the increase in the oxidation number of manganese from birnessite to todorokite, which in turn was due to the disproportionation of Mn^{3+} to Mn^{4+} and Mn^{2+} and to the ejection of some Mn^{2+} into the solution during the synthesis.[10]

The influence of uranium solution pH on the uptake of uranium

Un-autoclaved samples. The uptake of uranium from aqueous solution by octahedral manganese oxide materials was expected to be a complicated phenomenon related to the nature of the materials, as well as the aqueous chemistry of uranium.

To determine the affinity of Na-birnessite and its corresponding cation-exchanged forms towards the uptake of uranium as a function of pH, the uranium solution pH was adjusted by adding concentrated nitric acid or very dilute sodium hydroxide (10^{-3} M) to the solution prior to mixing. A contact time of 4 hours was chosen to ensure pH stability and establishment of equilibrium. The birnessites, and their autoclaved forms, were stable throughout the pH range of interest.

The uptake of uranium (Figs. 4a and b) increased with increasing uranium solution pH to reach a maximum at pH 2–6 and decreased sharply thereafter. Uranium sorption was at a maximum at pH 4 on the alkali metal exchanged forms, apart from K-birnessite which reached its maximum value at pH 2. The uptakes of uranium on alkaline earth and transition metal exchanged birnessite samples reached a maximum at pH 6, apart from Ba-birnessite (pH 4).

K-birnessite was the most effective material with a distribution factor of 1.14 × 10^5 mL g^{-1} at pH 2, concomitant with 100% sorption. The uranyl ion (UO_2^{2+}) was the most likely dominant species at this low solution pH.[31] Cs- and Co-birnessites had similar K_d values, 5.7 × 10^4 (at pH 4) and 5.6 × 10^4 mL g^{-1} (pH 6) respectively (100% sorption for both materials). A lower K_d for uranium sorption was observed for Ba-birnessite, *i.e.* 1.5 × 10^4 mL g^{-1} (99% sorption) at pH 4.

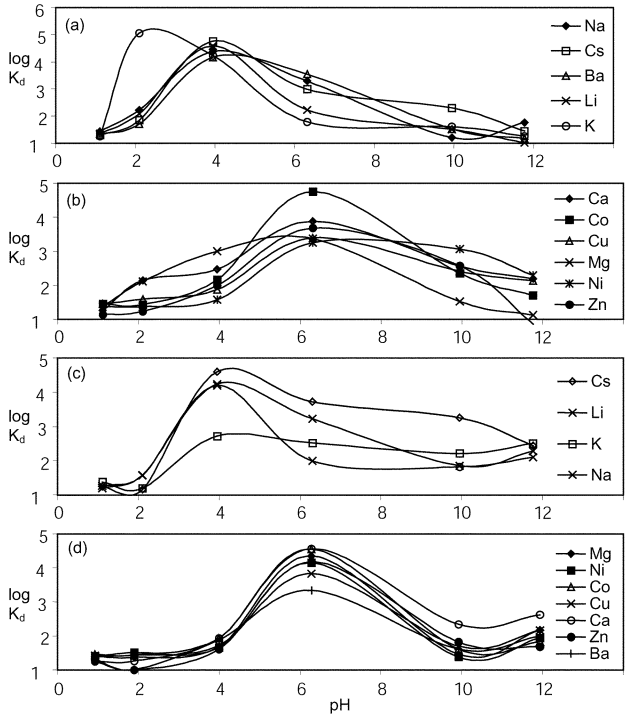

Fig. 4 Distribution coefficients of uranium sorption on non-autoclaved Na-birnessite, its cation-exchanged samples (a and b) and their autoclaved forms (c and d) as a function of uranium solution pH at ambient temperature (V/M = 200 mL g^{-1}, [U] = 250 mg L^{-1}).

The uptake of some species can be considered to take place whereby ion exchange occurs as cations penetrate into the internal structure through the micropores. The process is then limited by the nature of the cation initially present, which controls the ion-exchange capacity of the minerals, coupled with the nature of the dimensions of the micropores.

Previous investigations[32] found that the hydrolysis of the uranyl ion became extensive at pH ≅ 3, even at a fairly low uranium concentration solution. This hydrolysis will involve the formation of mononuclear species such as $[UO_2(OH)]^+$ as well as polynuclear ones, *e.g.* $[(UO_2)_2(OH)_2]^{2+}$, $[(UO_2)_3(OH)_5]^+$. In addition, the existence of $U_2O_5^{2+}$, $U_3O_8^{2+}$ and polymeric species of the type $UO_2(UO_3)_4^{2+}$ has been suggested. The uranyl ion concentration is around 50% at pH ∼ 4 and almost negligible[16] at higher pH. This means that it was conceivable that uranium was taken up by both ion exchange and surface sorption.

The uptake of uranium on Li-exchanged birnessite (Fig. 4a) increased with increasing solution pH, reaching a maximum K_d of 3.8 × 10^4 mL g^{-1} at pH 4 (99.5% sorption), and decreased sharply thereafter. K_d was 2.4 × 10^4 mL g^{-1} (99% sorption) in the case of Na-birnessite at the same pH.

Dyer *et al.*[20] studied the sorption of trace ^{137}Cs, ^{89}Sr, and ^{57}Co on Na- and K-exchanged birnessites across a wide pH range. They found that Na-birnessite was highly effective for the removal of trace cobalt as pH increased, becoming constant at pH 7–10 (K_d = 4.5 × 10^5 mL g^{-1}). It decreased thereafter.

In this study, the Ca-, Mg- and Ni-exchanged birnessites had K_d values of 7.6 × 10^3, 2.34 × 10^3 and 1.76 × 10^3 mL g^{-1} (100, 92 and 90% sorption), respectively, at pH 6 (Fig. 3b). K_d values did not exceed 70 mL g^{-1} (pH 3–3.5) in deionised water. The higher distribution factors at elevated pH could be ascribed to the predominance of surface sorption and precipitation rather than ion exchange.

Hydrolysis generally increases as the pH is lowered, and the exchanger may be converted to a hydrogen form. This could be accompanied by a structural change. Here the uranium solution pH varied significantly during the sorption experiments, but it was impossible to assess hydrogen ion uptake since these cations were also involved in the hydrolysis reactions of U(VI).[31] Suib and Carrodo[33] have reported that uranyl species were retained only on the external surface of natural scolecite, chabazite, heulandite and stilbite because the size of the uranyl ion (3.84 Å) prevented it from entering the relatively small pores of these zeolites.

Autoclaved birnessites. Study of the effect of uranium solution pH on uranium sorption of the autoclaved birnessite samples (Figs. 4c and 4d) revealed more or less identical trends to those of the un-autoclaved ones with maximum uptake occurring at pH 4 or 6. The distribution coefficients obtained, however, were less than those obtained on the un-autoclaved samples apart from those of Ca, Mg, and Ni autoclaved-birnessite. For instance, autoclaved K-birnessite had a K_d value only of 525 mL g^{-1} (72% sorption) at pH 4 whilst for untreated K-birnessite it was 1.14 × 10^5 mL g^{-1} (100% sorption) at pH 2.

Higher K_d values were obtained at pH ∼ 6 with autoclaved Ca-, Mg- and Ni-birnessite samples, 3.63 × 10^4 (99.5% sorption), 2.24 × 10^4 (99.1% sorption), and 1.41 × 10^4 mL g^{-1} (98.6% sorption) respectively. Although these materials produced lower K_d values in deionised water (pH 3–3.5) they gave much higher K_d values at pH 6 with high percentage sorption (98.6–99.5%). This indicated that uranium sorption again was probably aided by surface sorption and surface precipitation at higher pH.

Conclusions

The layered and tunnel manganese oxide materials studied herein showed different sorption properties for the uptake of uranium. A high distribution factor was found for uranium on un-autoclaved Cs-birnessite in deionised water, *ca.* 1.67×10^6 mL g^{-1} (100% sorption) after 2 hours' equilibrium time. Of the autoclaved materials, Li-exchanged birnessite yielded the best uptake of uranium with a K_d of 2.71×10^5 mL g^{-1}. At different uranium solution pH the sorption mechanism of uranium was a function of the aqueous chemistry of uranium as well as in of the structural features of the microporous materials used. Maximum distribution coefficients were obtained at pH 6 on alkaline earth and transition metal exchanged birnessites; and at pH 4 for alkali metal exchanged forms, apart from K-birnessite (pH = 2).

It seems that uranium uptake could take place *via* ion exchange when pH $\sim$ 3 and uranium was probably present as the uranyl cation. In contrast, at higher solution pH, when more complex species were present, sorption was more likely to be by surface sorption and precipitation.

Acknowledgement

We would like to thank the Atomic Energy Commission of Syria for the financial support to L. Al-Attar throughout her research work. Jon Newton is sincerely thanked for his help with plotting the graphs.

References

1 S. K. White, *J. Am. Water Works Assoc.*, 1983, **75**, 374.
2 Q. Feng, H. Kanoh, Y. Miyai and K. Ooi, *Chem. Mater.*, 1995, **7**, 1722.
3 L. H. P. Jones and A. A. Milne, *Mineral. Mag.*, 1956, **31**, 283.
4 J. W. Murray, *J. Colloid Interface Sci.*, 1974, **46**, 357.
5 P. LeGoff, N. Baffer, S. W. Bach and J. P. Pereiran-Ramous, *Mater. Res. Bull.*, 1996, **31**, 63.
6 A. T. Stone, K. L. Godtfredsen and B. Deng, in *Chemistry of aquatic systems: Local and global perspectives*, eds. G. Bidoglio and W. Stumm, 1994, p. 337, EURO courses series.
7 Q. Feng, H. Kanoh, Y. Miyai and K. Ooi, *Chem. Mater.*, 1995, **7**, 1226.
8 R. M. McKenzie, *Aust. J. Soil Res.*, 1967, **8**, 97.
9 D. C. Golden, J. B. Dixon and C. C. Chen, *Clays Clay Miner.*, 1986, **34**, 511.
10 D. C. Golden, C. C. Chen and J. B. Dixon, *Clays Clay Miner.*, 1987, **35**, 271.
11 Y. F. Shen, S. L. Suib and C. L. O'Young, *J. Am. Chem. Soc.*, 1994, **116**, 11020.
12 Y. F. Shen, R. P. Zerger, R. N. DeGuzman, S. L. Suib, L. McCurdy, D. I. Potter and C. L. O'Young, *Science*, 1993, **260**, 511.
13 Z. R. Tian, Y. G. Yin, S. L. Suib and C. L. O'Young, *Chem. Mater.*, 1997, **9**, 1126.
14 D. C. Golden, C. C. Chen and J. B. Dixon, *Science*, 1986, **231**, 717.
15 P. Misaelides, A. Godelitsas, A. Filippidis, D. Charistos and I. Anousis, *The Science of the Total Environment*, 1995, **173/174**, 237.
16 R. N. Sylva and M. R. Davidson, *J. Chem. Soc., Dalton Trans.*, 1979, 465.
17 A. Dyer, *Liquid Scintillation Counting Practice*, Heyden & Son, London, 1980.
18 D. Lide, *Handbook of Chemistry and Physics*, 75th edn., CRC Press Inc., Cleveland, Ohio, 1995.
19 R. G. Burns, V. M. Burns and H. W. Stockman, *Am. Mineral.*, 1983, **68**, 972.
20 A. Dyer, M. Pillinger, R. Harjula and S. Amin, *J. Mater. Chem.*, 2000, **10**, 1867.
21 V. A. Drits, E. Silvester, A. I. Gorshkov and A. Manceau, *Am. Mineral.*, 1997, **82**, 964; E. Silvester, A. Manceau and V. A. Drits, *Am. Mineral.*, 1997, **82**, 962.
22 L. Al-Attar, A. Dyer and R. Blackburn, *J. Radioanal. Nucl. Chem.*, 2000, **246**, 451.
23 L. Al-Attar and A. Dyer, *J. Radioanal. Nucl. Chem.*, 2001, **247**, 121.
24 R. Giovanoli and B. Balmer, *Chimica*, 1981, **35**, 53.
25 C. C. Chen, D. C. Golden and J. B. Dixon, *Clays Clay Miner.*, 1986, **34**, 565.
26 M. Tsuji, Y. Tanaka, M. Abe and Y. Tanaka, *New Development in Ion Exchange*, 1991, Kodansha, Ltd., Tokyo, p. 627.
27 M. Tsuji, M. Abe, Y. Tanaka and Y. Tanaka, *Seventh Symposium on Salt*, 1993, **Vol 2**, 23.
28 M. Tsuji and M. Abe, *Solvent Extr. Ion Exch.*, 1984, **2**, 253.
29 M. Tsuji and S. Komarneni, *J. Mater. Res.*, 1993, **8**, 611.
30 A. Dyer, M. Pillinger, J. Newton, R. Harjula, T. Moller and S. Amin, *J. Chem. Mater.*, 2000, **12**(12), 3798.
31 C. F. Baes, Jr. and R. E. Mesmer, *The Hydrolysis of Cations*, Krieger, Malabar, Florida, 1986.
32 J. A. Grindler, *The Radiochemistry of Uranium*, NAS-NS, Washington, 1962, p. 3050.
33 S. L. Suib and K. A. Carrado, *Inorg. Chem.*, 1985, **24**, 200.